Supporting Information

Fast dissolving eutectic compositions of two anti-tubercular drugs

Suryanarayan Cherukuvada and Ashwini Nangia*

School of Chemistry, University of Hyderabad, Prof. C. R. Rao Road, Central University PO, Gachibowli, Hyderabad 500 046, India

E-mail: ashwini.nangia@gmail.com

Table S1 Crystallographic parameters.

molecular adduct	PZA−SA	INH−SA[a]	PZA−FA	INH−FA	INH−FA
empirical formula	$(C_5H_5N_3O) \cdot (C_4H_6O_4)_{0.5}$	$(C_6H_7N_3O) \cdot (C_4H_6O_4)_{0.5}$	$(C_5H_5N_3O) \cdot (C_4H_4O_4)_{0.5}$	$(C_6H_7N_3O)_2 \cdot (C_4H_4O_4)$	$(C_6H_7N_3O)_2 \cdot (C_4H_4O_4)$
formula weight	182.16	196.19	181.16	390.36	390.36
crystal system	monoclinic	monoclinic	monoclinic	monoclinic	monoclinic
space group	$P2_1/n$	$P2_1/n$	$P2_1/n$	$P2_1/n$	$P2_1/n$
T/K	298(2)	298(2)	298(2)	298(2)	100(2)
a/Å	3.8701(4)	6.971(6)	3.7408(7)	8.1339(3)	7.883(2)
b/Å	17.3536(18)	19.508(17)	17.352(2)	8.7424(4)	8.697(3)
c/Å	12.4978(13)	7.260(6)	12.558(2)	12.4779(5)	12.506(4)
α/°	90	90	90	90	90
β/°	95.859(2)	114.603(13)	95.760(16)	96.933(4)	97.74(3)

γ/°	90	90	90	90	90
Z	4	4	4	4	4
V/Å^3	834.97(15)	897.7(13)	811.0(2)	880.81(6)	849.5(4)
D_{calc}/g cm^{-3}	1.449	1.452	1.484	1.472	1.526
μ/mm^{-1}	0.116	0.113	0.119	0.115	0.120
reflns collected	8467	9228	3083	3941	8546
unique reflns	1655	1784	1656	1794	1677
observed reflns	1433	1563	1194	1512	1557
$R_1[I > 2\sigma(I)]$	0.0424	0.0486	0.0520	0.0366	0.0397
wR_2 [all]	0.1038	0.1301	0.1146	0.0897	0.0942
goodness-of-fit	1.056	1.085	1.040	1.052	1.114
diffractometer	Bruker Smart-Apex	Bruker Smart-Apex	Oxford Xcalibur Gemini	Oxford Xcalibur Gemini	Bruker Smart-Apex

[a] Lemmerer et al.[13d] reported this crystal structure data collected at 173 K

Table S2 Hydrogen bonds in crystal structures of molecular adducts.

Interaction	H···A/ Å	D···A/ Å	∠D–H···A/ º	Symmetry code
PZA−SA				
O2–H2···N3	1.80(2)	2.700(2)	174(2)	[a]
N1–H1A···O2	2.31(2)	3.053(2)	140(2)	3/2–x, 1/2+y, 1/2–z
N1–H1B···O1	1.96(2)	2.910(2)	173(2)	1–x, 1–y, –z

N1–H1A···N2	2.30(2)	2.720(2)	108(1)	[b]
C5–H5···O3	2.61	3.272(2)	128	[a]
C3–H3···O3	2.53	3.438(2)	164	3/2+x, 1/2–y, 1/2+z
C4–H4···O1	2.39	3.304(2)	169	1/2+x, 1/2–y, 1/2+z
INH−SA				
O3–H3A···N3	1.66(3)	2.621(3)	171(3)	[a]
N1–H1A···O1	2.24(3)	3.008(3)	146(2)	–x, –y, 1–z
N1–H1B···O3	2.29(3)	3.120(3)	152(2)	–x, –y, 1–z
N2–H2···N1	2.16(2)	2.940(3)	152(2)	1–x, –y, 1–z
C4–H4···O2	2.32	3.128(3)	144	–1/2+x, 1/2–y, –1/2+z
C5–H5···O2	2.72	3.339(3)	125	[a]
PZA−FA				
O2–H2···N3	1.74(3)	2.686(2)	174(3)	[a]
N1–H1A···O2	2.27(3)	3.073(3)	140(2)	1/2–x, –1/2+y, 1/2–z
N1–H1B···O1	1.93(3)	2.913(3)	172(2)	1–x, –y, 1–z
N1–H1A···N2	2.29(3)	2.726(3)	107(2)	[b]
C5–H5···O3	2.56	3.224(2)	128	[a]
C3–H3···O3	2.44	3.344(2)	163	–3/2+x, 1/2–y, –1/2+z
C4–H4···O1	2.38	3.304(3)	171	–1/2+x, 1/2–y, –1/2+z
INH−FA[c]				

O3···H3A···N3	1.22(2), 1.33(3)	2.542(2)	172(2)	[a]
N1–H1A···O1	2.30(2)	3.048(2)	142(2)	1/2+x, 3/2–y, –1/2+z
N1–H1B···O3	2.28(2)	3.047(2)	143(2)	3/2–x, 1/2+y, 3/2–z
N2–H2···O2	2.01(2)	2.873(2)	163(2)	x, –1+y, z
C4–H4···O2	2.86	3.439(2)	121	[a]
C4–H4···N1	2.67	3.534(2)	155	x, –1+y, z
C5–H5···O1	2.61	3.500(2)	161	–1/2+x, 3/2-y, 1/2+z
C6–H6···O2	2.57	3.353(2)	142	x, 1+y, z
INH–FA[d]				
O3···H3A···N3	1.30(3), 1.23(3)	2.523(2)	171(2)	[a]
N1–H1A···O1	2.19(2)	3.015(2)	148(2)	–1/2–x, 3/2+y, 3/2–z
N1–H1B···O3	2.20(2)	2.987(2)	146(2)	–3/2+x, 5/2–y, 1/2+z
N2–H2···O2	2.00(2)	2.832(2)	163(2)	x, –1+y, z
C4–H4···O2	2.77	3.365(2)	121	[a]
C4–H4···N1	2.62	3.503(2)	154	x, –1+y, z
C5–H5···O1	2.52	3.432(2)	162	–1/2+x, 3/2-y, 1/2+z
C6–H6···O2	2.55	3.341(2)	141	x, 1+y, z

[a] Molecules in the same asymmetric unit

[b] Intramolecular hydrogen bond.

[c] 298 K data

[d] 100 K data

Table S3 X-ray powder diffraction pattern of PZA, INH and binary PZA–INH eutectic.

PZA			PZA–INH			INH		
Angle 2θ (°)	d spacing (Å)	Relative Intensity (%)	Angle 2θ (°)	d spacing (Å)	Relative Intensity (%)	Angle 2θ (°)	d spacing (Å)	Relative Intensity (%)
7.9	11.1	67.2	7.8	11.3	42.7	10.0	8.9	5.1
13.9	6.3	15.4	9.8	9.0	4.0	12.1	7.3	31.3
15.5	5.7	59.7	11.9	7.4	14.9	14.5	6.1	68.8
15.8	5.6	54.5	13.7	6.4	10.8	15.8	5.6	50.4
17.7	5.0	100.0	14.3	6.2	13.5	16.8	5.2	98.3
20.6	4.3	10.4	15.3	5.8	40.9	19.8	4.5	40.6
23.8	3.7	15.9	15.6	5.7	71.6	24.1	3.7	21.2
24.5	3.6	15.9	16.7	5.3	64.1	24.3	3.6	12.4
26.5	3.3	45.3	17.6	5.0	67.7	25.3	3.5	81.1
27.6	3.2	80.3	19.6	4.5	12.9	26.2	3.4	51.3
29.2	3.0	8.7	20.5	4.3	6.1	27.4	3.2	100.0

29.7	3.0	5.5	23.6	3.7	12.0	28.8	3.1	18.4
31.1	2.9	6.4	23.9	3.7	12.0	29.0	3.0	30.3
31.7	2.8	8.1	24.1	3.7	11.4	29.6	3.0	12.6
32.2	2.8	7.3	24.3	3.6	9.5	30.7	2.9	9.8
			25.2	3.5	58.5	32.3	2.7	12.4
			26.1	3.4	39.5			
			27.2	3.2	100.0			
			28.7	3.1	12.9			
			29.4	3.0	9.5			
			30.5	2.9	6.9			
			32.1	2.8	12.1			

Table S4 X-ray powder diffraction pattern of ternary PZA–SA–INH eutectic and binary PZA–SA and INH–SA cocrystals.

PZA–SA			PZA–SA–INH			INH–SA		
Angle 2θ (°)	d spacing (Å)	Relative Intensity (%)	Angle 2θ (°)	d spacing (Å)	Relative Intensity (%)	Angle 2θ (°)	d spacing (Å)	Relative Intensity (%)
8.6	10.2	8.8	8.4	10.5	6.4	8.9	9.9	4.1
12.3	7.1	17.5	12.1	7.3	7.2	14.6	6.0	10.1

14.1	6.2	8.3	14.4	6.1	7.7	15.3	5.7	13.3
15.0	5.8	34.0	14.7	5.9	18.1	16.4	5.3	58.2
17.4	5.0	67.6	15.1	5.8	9.6	17.2	5.1	20.0
20.9	4.2	55.5	16.2	5.4	40.1	22.8	3.9	12.4
21.5	4.1	7.9	17.2	5.1	34.0	23.3	3.8	17.7
23.4	3.8	30.9	20.6	4.3	30.8	24.7	3.6	20.4
25.2	3.5	34.0	21.3	4.1	6.8	24.9	3.5	16.5
25.5	3.4	21.9	22.5	3.9	12.7	26.1	3.4	22.2
26.3	3.3	100.0	23.1	3.8	34.0	26.8	3.3	100.0
29.9	2.9	23.9	24.6	3.6	24.1	27.2	3.2	26.1
30.9	2.8	8.3	24.9	3.5	21.4	29.3	3.0	5.7
31.6	2.8	11.5	25.2	3.5	17.0	30.6	2.9	11.3
32.3	2.7	11.1	26.0	3.4	76.7	33.4	2.6	3.8
33.5	2.6	11.3	26.5	3.3	100.0			
			26.9	3.3	28.3			
			29.6	3.0	21.4			
			30.4	2.9	17.0			
			31.3	2.8	14.0			
			32.1	2.7	12.6			
			33.2	2.6	13.5			

Table S5 X-ray powder diffraction pattern of ternary PZA–FA–INH eutectic and binary PZA–FA and INH–FA cocrystals.

PZA–FA			PZA–FA–INH			INH–FA		
Angle 2θ (°)	d spacing (Å)	Relative Intensity (%)	Angle 2θ (°)	d spacing (Å)	Relative Intensity (%)	Angle 2θ (°)	d spacing (Å)	Relative Intensity (%)
8.9	9.9	9.0	8.8	10.0	8.7	12.5	7.1	10.1
12.5	7.1	24.1	12.5	7.1	14.3	14.5	6.1	6.6
14.2	6.2	12.7	14.2	6.2	17.2	16.2	5.5	34.1
15.2	5.8	47.4	14.8	5.9	13.2	16.9	5.2	13.1
17.5	5.0	84.1	15.2	5.8	22.5	17.6	5.0	12.2
18.9	4.7	8.4	15.6	5.7	20.3	19.9	4.5	44.8
21.0	4.2	65.0	16.1	5.5	22.2	21.8	4.1	18.8
21.7	4.1	10.4	16.7	5.3	47.4	22.2	4.0	8.1
22.9	3.8	5.7	17.6	5.0	34.9	23.0	3.8	18.5
24.2	3.7	29.6	18.1	4.9	18.3	23.3	3.8	19.9
25.0	3.5	11.0	18.9	4.7	20.3	24.4	3.6	20.9
26.1	3.4	40.6	19.9	4.4	21.1	25.6	3.5	100.0
26.3	3.4	29.1	21.0	4.2	32.5	26.3	3.4	39.3
27.0	3.3	100.0	21.7	4.1	16.8	27.4	3.2	20.6

28.4	3.1	16.1	23.5	3.8	31.8	27.9	3.2	49.5
29.4	3.0	11.5	25.4	3.5	59.6	28.9	3.1	22.6
30.5	2.9	24.8	26.6	3.3	81.1	29.8	3.0	39.3
30.8	2.9	12.8	26.9	3.3	100.0	31.5	2.8	4.7
31.7	2.8	11.8	27.4	3.2	41.5	32.3	2.7	5.7
32.2	2.7	11.6	27.9	3.2	37.4			
			28.4	3.1	33.4			
			29.5	3.0	28.6			
			29.7	3.0	29.3			
			30.8	2.9	18.0			
			32.4	2.7	14.3			

Table S6 ^{15}N SS-NMR chemical shifts (δ, ppm scale) of the compounds.

PZA (pure)	INH (pure)	PZA–INH (eutectic)	PZA–SA (cocrystal)	INH–SA (cocrystal)	PZA–SA–INH (eutectic)	PZA–FA (cocrystal)	INH–FA (cocrystal)	PZA–FA–INH (eutectic)
–29.9 (N3-non intramolecular hydrogen bonded pyrazine N)	–42.1 (N6-pyridine N)	–251.9 (N5)	–72.8 (N3)	–92.3 (N6)	–73.4 (N3)	–280.2 (N1)	–121.4 (N6)	–121.4 (N6)
–279.1 (N1-Amide NH_2)	–252.3 (N5-hydrazide secondary amine)	–279.2 (N1)	–280.2 (N1)	–253.9 (N5)	–91.1 (N6)		–250.4 (N5)	–250.0 (N5)
	–322.5 (N4-hydrazide primary amine)	–321.9 (N4)		–324.5 (N4)	–252.8 (N5)		–327.8 (N4)	–278.1 (N1)
					–280.4 (N1)			–327.0 (N4)
					–324.6 (N4)			

Table S7 FT–IR spectral bands of compounds.

IR vibration	PZA (pure)	INH (pure)	SA (pure)	FA (pure)	PZA–INH (eutectic)	PZA–SA (cocrystal)	INH–SA (cocrystal)	PZA–SA–INH (eutectic)	PZA–FA (cocrystal)	INH–FA (cocrystal)	PZA–FA–INH (eutectic)
N–H (stretch)	3414, 3162	3304, 3111	---	---	3412, 3302, 3162, 3111	3424, 3169	3303, 3220	3425, 3304, 3219	3426, 3183	3323, 3166	3403, 3325, 3219
O–H (stretch)	---	---	3037	3083	---	2932	2933	2937	2810	2819	2810
C=O (stretch)	1716	1667	1731, 1693	1675	1715, 1668	1712	1708, 1682	1709, 1681	1710, 1693	1681	1712, 1682
N–H (bend)	1611	1635, 1602	---	---	1635, 1611	1610	1635, 1609	1635, 1609	1603	1637, 1581	1638
O–H (bend)	---	---	1419	1426	---	1420	1426	1427	1434	1414	1413
C–N (stretch)	1379	1412	---	---	1412, 1379	1380	1410	1409, 1382	1383	1323	1377
C–O (stretch)	---	---	1310	1320	---	1325	1331	1325	1313		1321

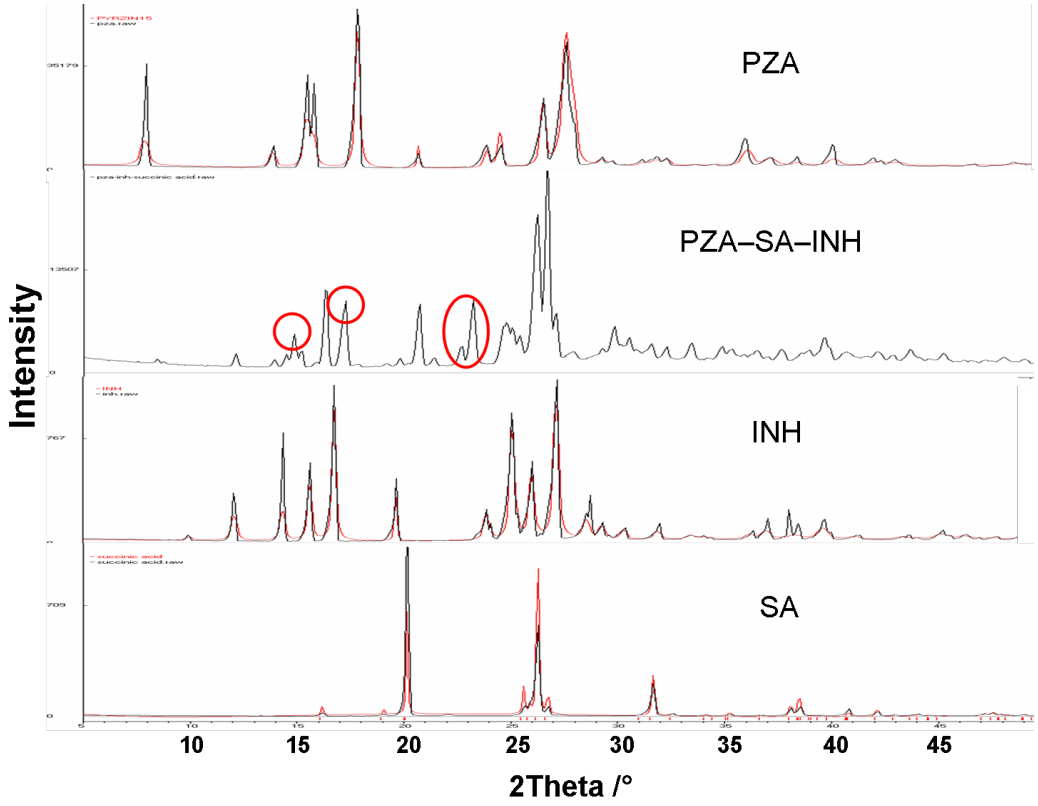

(a)

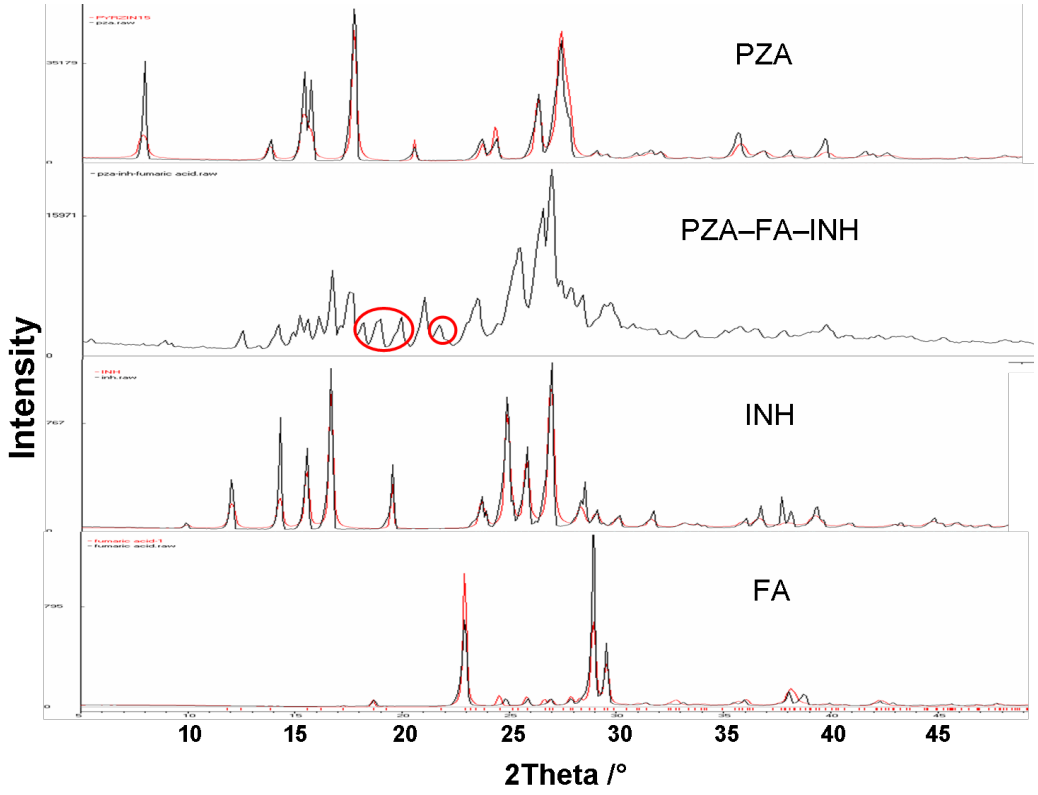

(b)

Figure S1 Comparison of the PXRD pattern of (a) ternary eutectic PZA–SA–INH with that of PZA, INH and SA and of (b) ternary eutectic PZA–FA–INH with that of PZA, INH and FA. Red circles indicate new and distinct diffraction peaks. The experimental PXRD patterns (black) of the pure compounds overlay peak-to-peak on the calculated lines (red) from the crystal structures.

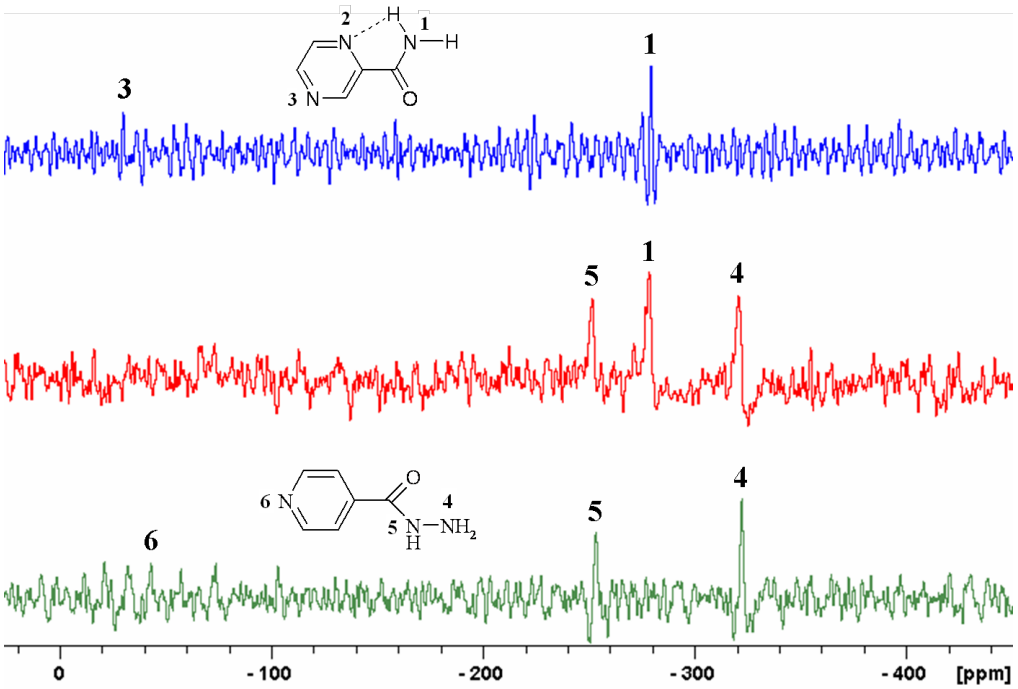

Figure S2 Comparison of the ^{15}N ss-NMR spectrum of binary PZA–INH eutectic (red) with that of PZA (blue) and INH (green). Aromatic nitrogens are weakly resolved but assigned with respect to side bands. The intramolecular hydrogen bonded pyrazine N of PZA could not be detected even after over 24 h of FID acquisition. The quality of spectra is marginal but a few lines are visible.

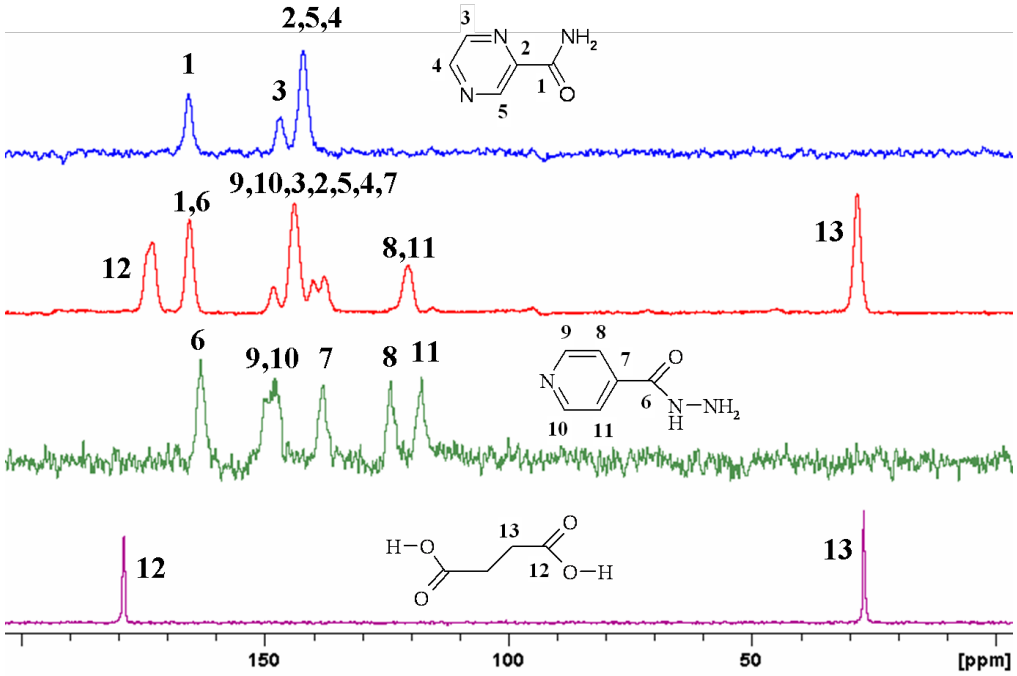

(a)

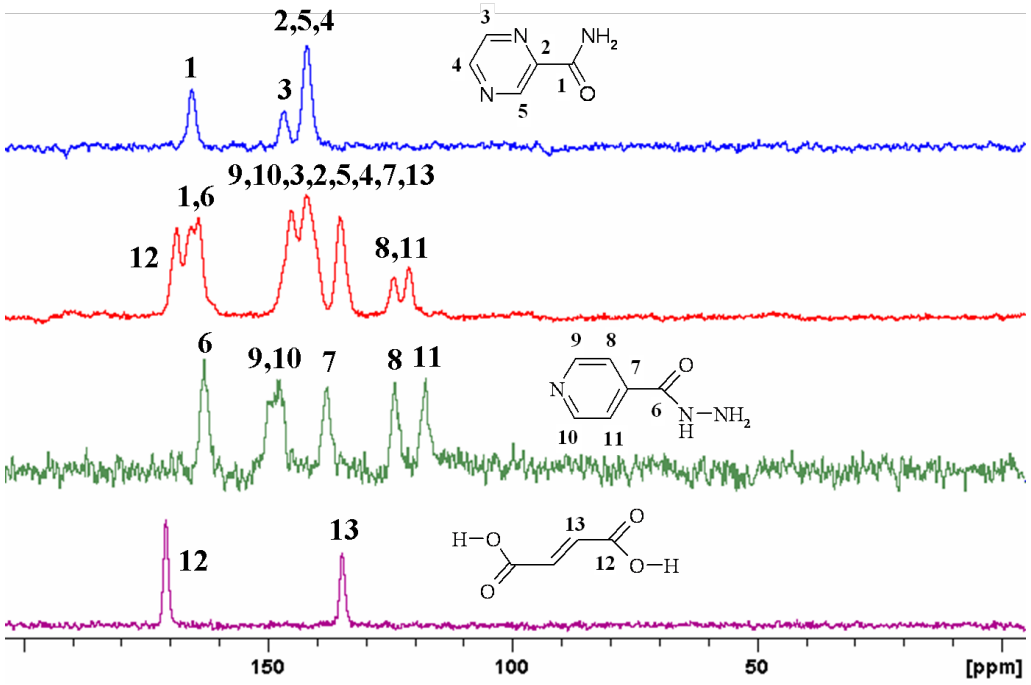

(b)

Figure S3 ^{13}C ss-NMR spectrum of (a) ternary PZA–SA–INH eutectic (red), PZA (blue), INH (green), and SA (purple), and (b) ternary PZA–FA–INH eutectic (red), PZA (blue), INH (green), and FA (purple). A few closely spaced resonances have merged to give a broad peak.

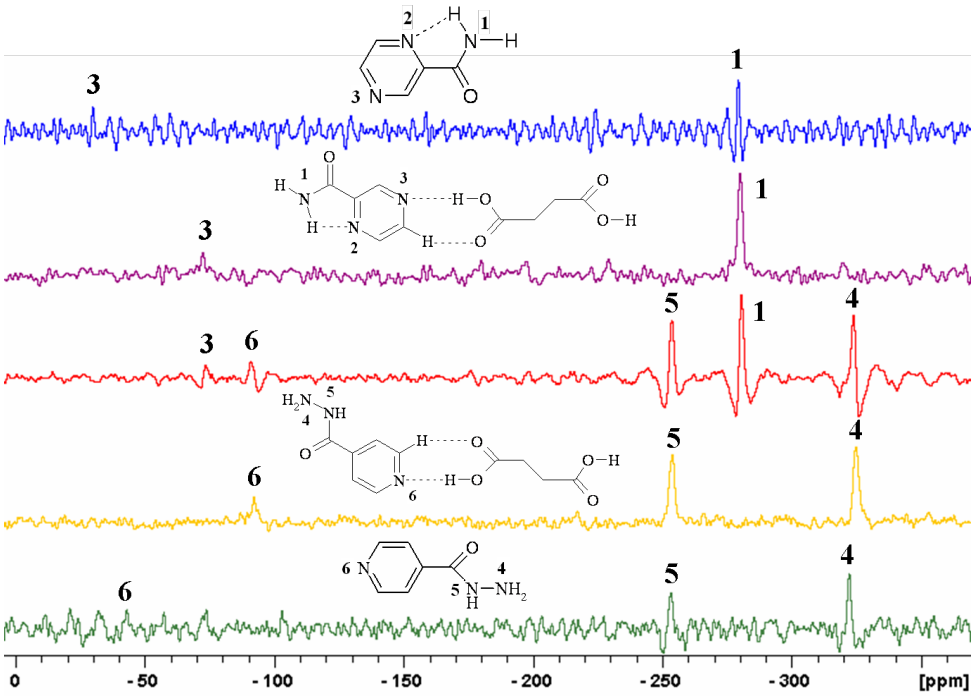

(a)

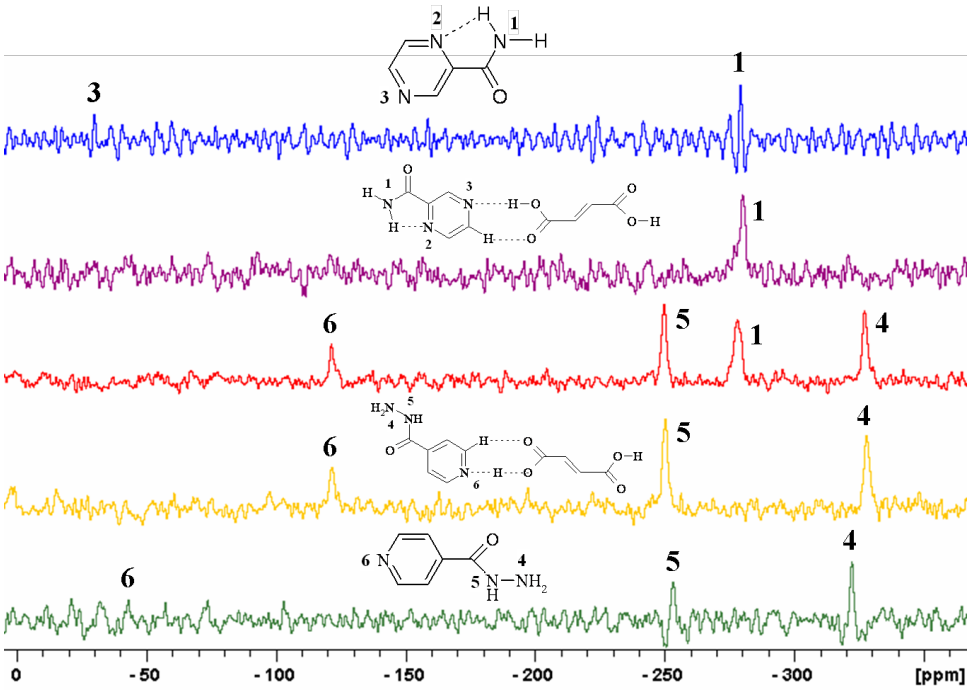

(b)

Figure S4 ^{15}N ss-NMR spectrum of (a) PZA (blue), PZA–SA cocrystal (purple), PZA–SA–INH eutectic (red), INH–SA cocrystal (yellow), and INH (green), and (b) PZA (blue), PZA–FA cocrystal (purple), PZA–FA–INH eutectic (red), INH–FA cocrystal (yellow), and INH (green). Aromatic nitrogens peaks are weakly resolved.

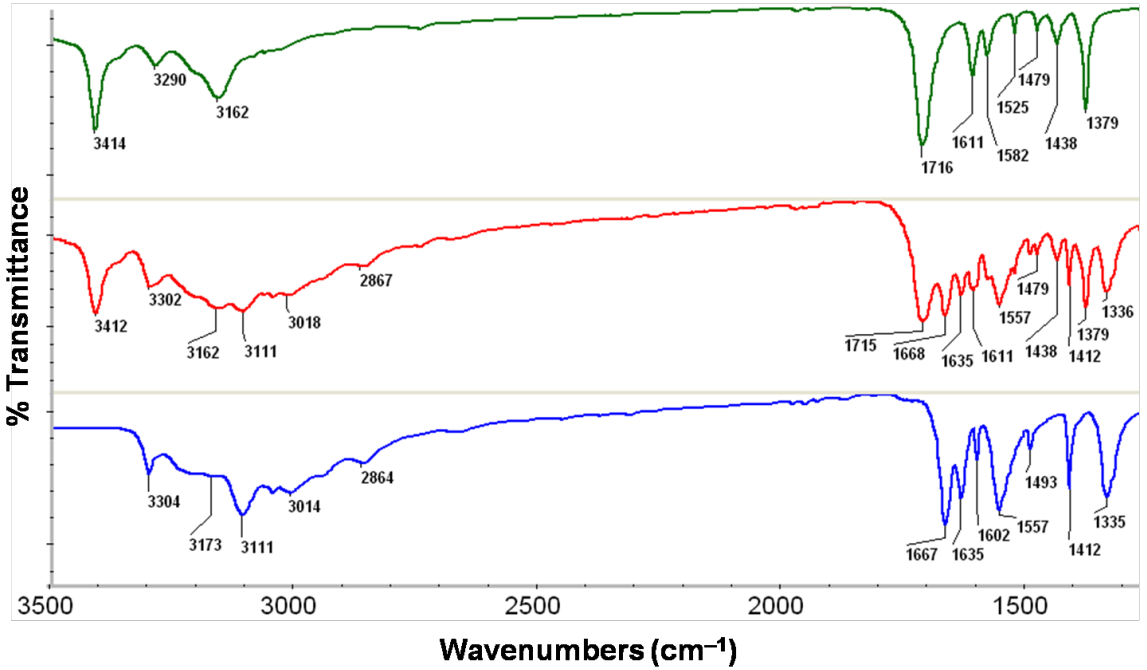

Figure S5 FT-IR spectrum of (a) binary PZA–INH eutectic (red), and PZA (green) and INH (blue). There is no shift in the vibrations frequency of eutectic compared to the pure drugs, indicating no cocrystal formation.

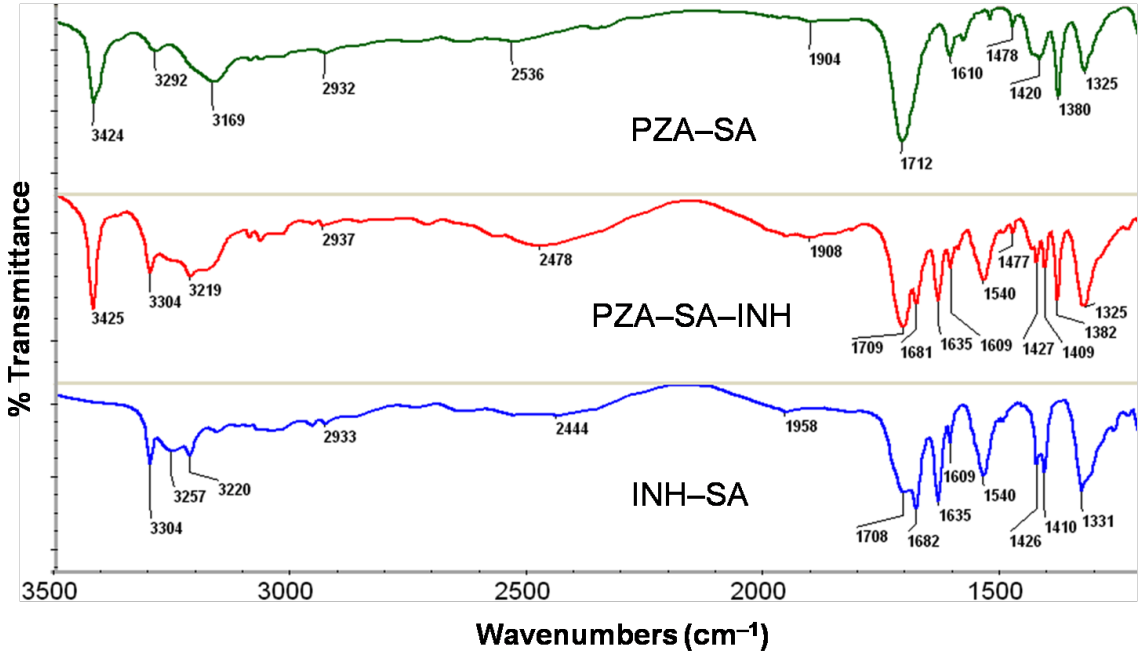

(a)

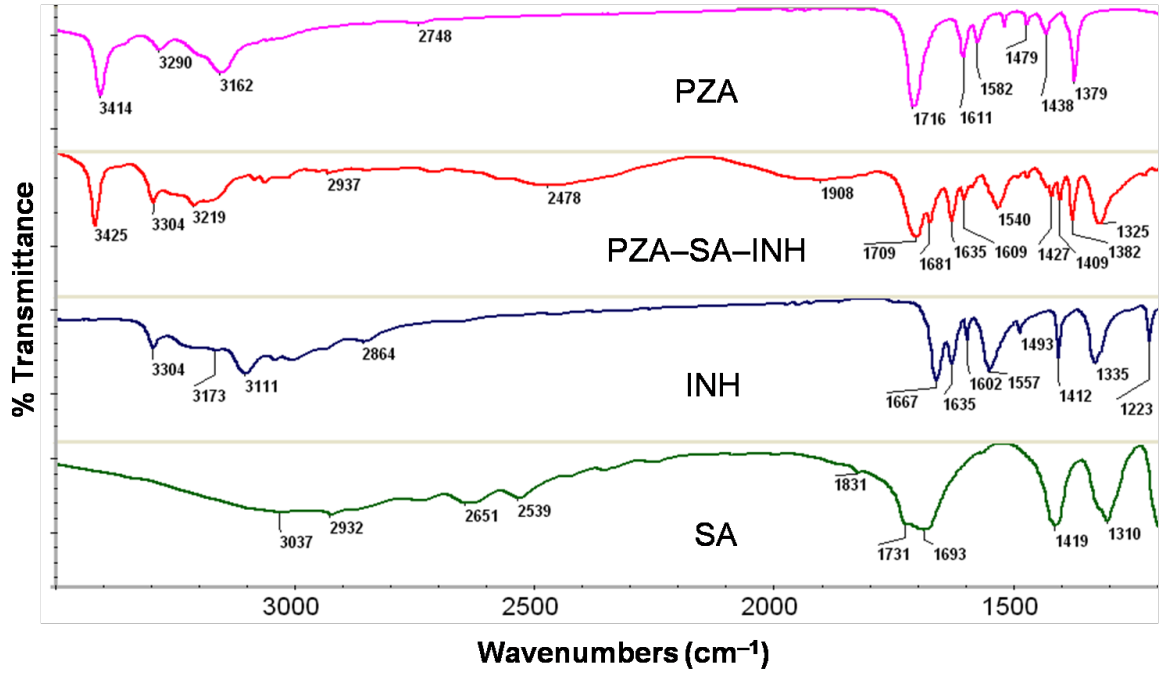

(b)

Figure S6 FT-IR spectrum of (a) PZA−SA−INH eutectic (red), PZA−SA (green), and INH−SA (blue), and (b) PZA–SA–INH eutectic (red), PZA (magenta), INH (blue), and SA (green). The C=O, O–H, N–H and C–N vibrations in the ternary eutectic match with the peaks for binary cocrystals and are different from those of the pure compounds (Table S7). Broad peaks at 2500 and 1900 cm^{-1} attributed to neutral O–H···N hydrogen bond (J. P. Castaneda et al., *J. Mol. Struct.*, 2003, **660**, 25; C. B. Aakeröy et al., Cr*ystEngComm.*, 2006, **8**, 586) were observed in the complexes PZA–SA−INH (2478, 1908 cm^{-1}), PZA−SA (2536, 1904 cm^{-1}) and INH–SA (2444, 1958 cm^{-1}) but not the parent drugs.

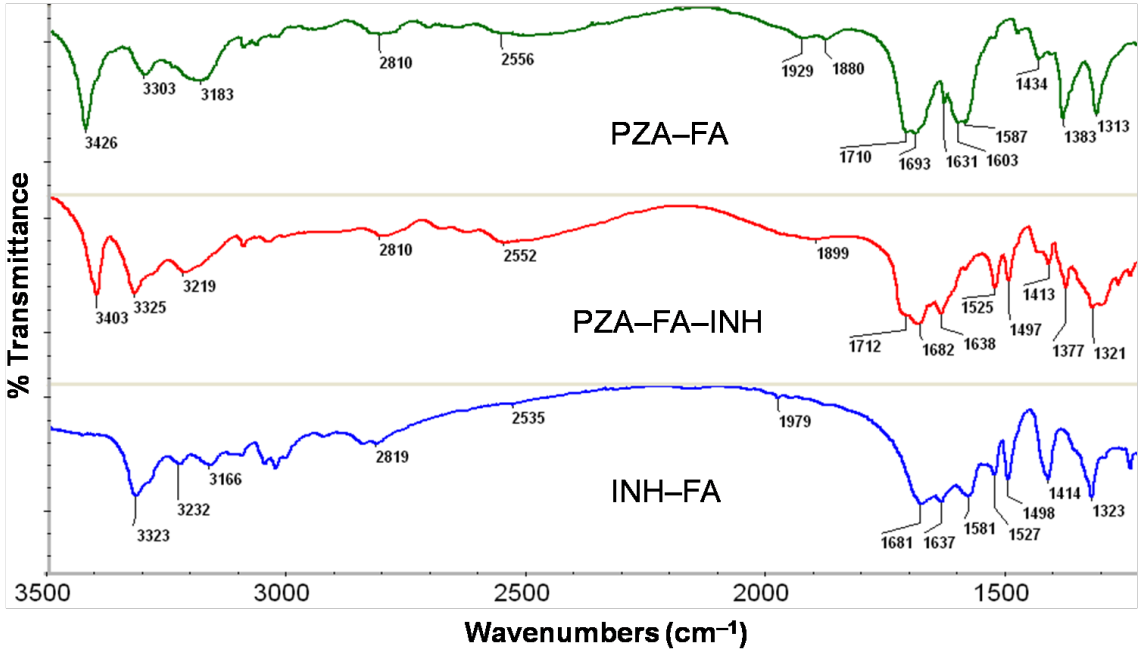

(a)

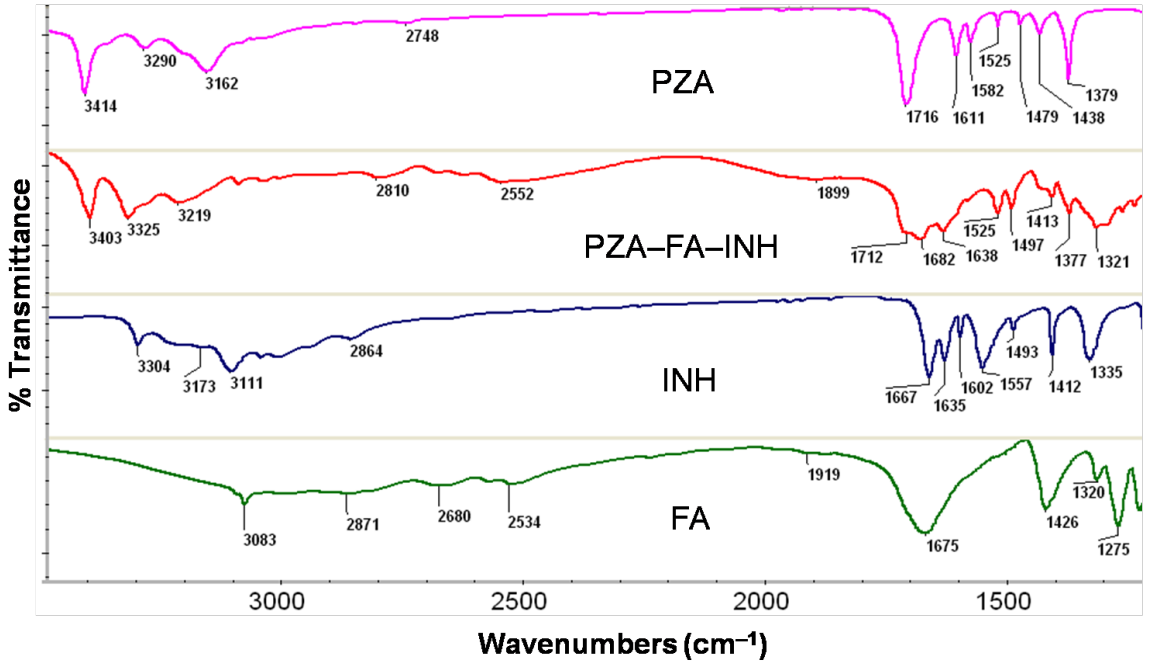

(b)

Figure S7 FT-IR spectrum of (a) PZA−FA−INH eutectic (red), PZA−FA (green), and INH−FA (blue), and (b) PZA–FA–INH eutectic (red), PZA (magenta), INH (blue), and FA (green). The C=O, O–H, N–H and C–N vibrations in the ternary eutectic matched with the peaks for the binary cocrystals and different from that of the parent compounds (Table S7). INH−FA shows very weak peaks at 2535, 1979 cm^{-1} supporting it to be a mixed ionization state as confirmed from its X-ray crystal structure (see Figure 1d).